Journal of Neuro-Oncology **22**: 191–200, 1994.

Laboratory Investigation

A rat glioma model, CNS-1, with invasive characteristics similar to those of human gliomas: A comparison to 9L gliosarcoma

Carol A. Kruse,[1,2] Michael C. Molleston,[3,4] Elizabeth P. Parks,[3] Patric M. Schiltz,[1] Bette K. Kleinschmidt-DeMasters[2] and William F. Hickey[3]
University of Colorado Health Sciences Center, Departments of [1] Surgery and [2] Pathology, Denver, Colorado and Dartmouth Medical Center, [3] Department of Pathology, Lebanon, New Hamsphire, [4] Present address: Texas Children's Hospital, Department of Neurosurgery, Houston, TX 77030, USA

Key words: brain tumor, glioblastoma, astrocytoma, rat tumor model, immunotherapy, infiltration, invasion

Summary

A glioma cell line, CNS-1, was developed in the inbred Lewis rat to obtain a histocompatible astrocytoma cell line with infiltrative and growth patterns that more closely simulate those observed in human gliomas. Rats were given weekly intravenous injections for a six month period with N-nitroso-N-methylurea to produce neoplasm in the central nervous system. Intracranial tumor was isolated, enzymatically and mechanically digested, and placed into culture. The tumor cell line injected subcutaneously on the flanks of Lewis rats grew extensively *in situ* as cohesive tumor masses but did not metastasize. Intracranially, CNS-1 demonstrated single cell infiltration of paranchyma and leptomeningeal, perivascular, and periventricular spread with expansion of the tumor within choroid plexus stroma. CNS-1 cells titrated in right frontal brain of Lewis rats at 10^5, 5×10^5, 10^5, 5×10^4 cells per group had mean survival times ranging from 20.5 to 30.2 days. CNS-1 was immunoreactive for glial fibrillary acidic protein, S100 protein, vimentin, neural cell adhesion molecule, retinoic acid receptor α, intercellular adhesion molecule, and neuron specific enolase. The CNS-1 cells commonly had one or more trisomies of chromosomes 11, 13 or 18; losses, possibly random, of chromosomes (3, 5, 19, 30, X or Y) were noticed, and a marker chromosome made up of approximately 3 chromosomes was usual. Comparisons of CNS-1 to 9L gliosarcoma tumor were made. The glial CNS-1 tumor model provides an excellent system in which to investigate a variety of immunological therapeutic modalities. It spreads within brain in a less cohesive mass than 9L and is accepted without rejection in non-central nervous system sites by Lewis rats.

Introduction

Glial neoplasms are among the most resistant tumors to conventional antineoplastic therapy. Surgery, radiation and chemotherapy are all palliative; none successfully eradicate the malignancy [1]. The reason for this is perhaps partially related to the growth characteristics of such primary central nervous system tumors. While they typically occur as a single mass lesion, the margins of the tumor are often ill-defined and characterized by individual infiltrative tumor cells. Few are microscopically sharply demarcated. Thus, if cure is to occur, the therapeutic regimen must not only eradicate the bulk of the tumor, it must eliminate the small groups of infiltrating cells that disseminate from the main tumor mass.

Few of the currently available rat brain tumor models optimally simulate the infiltration and growth patterns observed in human gliomas. Frequently they lack the diffuse individual cell infiltration patterns typical of human gliomas, growing in-

stead like well demarcated brain metastases or sarcomas. Such a limitation is particularly disadvantageous when animal brain tumor models are used to study immunotherapeutic regimens which need to assess the ability of cytotoxic cells or antibodies to reach and eradicate individually infiltrating glioma cells. In addition, minor histocompatibility antigen differences between the host and the tumor cells can result in rejection of the test tumor, confounding ones ability to carefully examine the efficacy of immunotherapeutic modalities in the test system.

The rat brain tumor models most commonly used have either been created by transformation of cells with Rous sarcoma virus, by injections of rats with various mutagenic agents such as methylcholanthrene or nitrosoureas, or by radiation [2, 3]. Among those more widely used are RT2, T9, C6, and 9L. The 9L rat gliosarcoma was induced in Fischer rats by weekly iv injection of N-nitrosomethylurea [3, 4]. Selection for the sarcomatous cell of this mixed gliosarcoma tumor type has occurred upon many culture passages.

A variety of approaches to the immunotherapy of gliomas has been attempted [5]. The immune system has the potential for locating disseminated antigen in tissues and eliminating it. For this reason, pursuing the refinement of adjuvant cellular therapy approaches is theoretically warranted, especially for non-sharply demarcated primary brain tumors where complete surgical resection might not be possible. Our laboratory has used the 9L gliosarcoma model established in the inbred, immunogenetically-characterized Fischer rat for our immunotherapy studies [6–10]. We chose the 9L model over the C6 glioma model, which was established in the outbred Sprague-Dawley rat, in view of the requirement for major histocompatibility characterization. It is particularly advantageous to know the specific haplotype of the rats when testing syngeneic or allogeneic cytotoxic T cells in adoptive immunotherapy regimens [6, 10]. This report examines the novel CNS-1 Lewis rat derived glioma cell line and compares its characteristics to the 9L gliosarcoma line.

Methods

Animals

Inbred specific pathogen free and viral antigen free Lewis (haplotype $RT1^l$) rats were purchased from Charles River Breeding Laboratories. All animals were male rats weighing 200–250 gm. Animals were injected intravenously weekly for a six month period with N-nitroso-N-methylurea (NMU # N-1517, Sigma, St. Louis, MO) to produce neoplastic disease in the central nervous system. Animals were observed daily from six months onward for evidence of gross neurological abnormalities.

Cells

9L gliosarcoma cells were cultured in RPMI 1640:Dulbecco's modified Eagle's medium (2:1 v/v) containing 10% fetal calf serum (Gibco, Grand Island, NY), 200 mM L-glutamine, 100 U/ml penicillin, and 0.1 mg/ml streptomycin.

A single cell suspension of CNS-1 cells were prepared from a primary intracranial tumor by enzymatic and mechanical digestion. Briefly, the tumor in Hank's Balanced Salt Solution (HBSS, Mediatech, Washington, DC) was minced into 1 to 2 mm pieces. To this mixture, concentrated enzymes were added so that the final concentrations were 0.002% DNase type I (Sigma), 0.01% hyaluronidase type V (Sigma), and 0.1% collagenase type IV (Sigma). The tissue was further dissociated by mechanical stirring for 1 to 2 hours at 37° C. The resulting suspension was washed twice with HBSS. The resulting cells were grown in RPMI 1640 medium (MA Whitaker Biologicals, Walkersville, MD) with 200 mM L-glutamine, 100 U/ml penicillin, 0.1 mg/ml streptomycin, and 10% fetal calf serum at a final pH of 7.2. The cells that attached to the plastic were passaged when confluent by dissociating the cells with 0.025% trypsin-EDTA in phosphate buffered saline (PBS, 45 mM Na_2HPO_4, 5 mM NaH_2PO_4, pH 7.4, and 0.15 M NaCl).

Immunocytochemistry

For immunostaining, tissues with tumor were placed into Tissue-Tek OCT embedding medium (Miles, Inc., Elkhart, IN), frozen on dry ice, then 5 μ sections placed onto polylysine-coated slides. Alternatively, tissue culture grown tumor cells were prepared either as cytospins of passaged cells, or they were plated onto tissue culture chamber/slides (Lab-Tek Products, Naperville, IL) and cultured until semi-confluency was reached. The medium was removed and the cells washed three times with PBS. The cells were fixed with acetone:methanol:37% formalin (45:45:10 v/v/v) at 0° C for ten minutes, rinsed with PBS and stored overnight at 4° C. One slide was stained with Harris hematoxylin; the others were stained by the alkaline phosphatase/anti-alkaline phosphatase technique [11] or by peroxidase/anti-peroxidase techniques according to manufacturer's instructions (Sternberger-Meyer Immunocytochemicals, Inc., Jarretsville, MD). Negative controls consisted of cultured cells incubated with irrelevant isotype antibody substituted for primary antibody; controls showed only rare nonspecific uptake of substrate by degenerating cells.

In some cases, cells grown on slides were fixed for 30–60 sec in absolute MeOH at – 20° C. Following this, they were extensively rinsed with 0.5 M Tris buffer at pH 7.6 and then overlaid with an appropriate primary antibody. The remainder of the method utilized the avidin-biotin complex system previously detailed [12]. Stains were considered positive only in the presence of an appropriately negative control.

The antibodies used and their sources were: rabbit polyclonals A587 to neuron specific enolase and the Z311 to S100 protein, the V9 polyclonal to vimentin, the M762 antibody to neurofilament, and the Z334 antibody to glial fibrillary acidic protein all from DAKO (Santa Barbara, CA); the 9,10α (F1) monoclonal antibodies to retinoic acid receptor α from Dr. P. Chambon, INSERM (Strasbourg, FR); the 3F4 monoclonal antibody to rat neuronal cell adhesion molecule (NCAM) from Dr. Susan L. Haines at the Childrens Hospital Research Foundation (Cincinnati, OH); and the 1A29 monoclonal antibody to rat intercellular adhesion molecule (ICAM-1) from Dr. C. Wayne Smith at Baylor College of Medicine (Houston, TX).

Karyotypic analyses

In preparation for cytogenetics, a 25 cm^2 flask of cells was transferred to four 25 cm^2 flasks. Two hours prior to processing the cells, colcemid and ethidium bromide were added to the medium [11]. Cells were processed at 2, 3 and 4 days. Slides were prepared and chromosomes were trypsin banded. Approximately 25 CNS-1 and 6 9 L cells were counted. A Genevision Karyotyping System (Applied Imaging, Pittsburgh, PA) was used to facilitate the identification of chromosomes by computer-assisted enhancement. Chromosomes from a Sprague-Dawley rat parotid cell line, 2RS, were used to obtain a normal karyotype; banding was compared to the rat chromosome idiogram of the Norway rat, *Rattus norvegicus* [13].

In vivo *titration of tumor*

Four experimental groups of animals received tumor cells intracranially by Hamilton syringe [6]. They were stereotactically injected at a point 3 mm lateral to midline, 2 mm anterior to bregma, at a 4 mm depth into right frontal cortex. 9 L tumor cells or CNS-1 tumor cells at various concentrations were slowly infused in a 10 μl volume. Bone wax was used to seal the hole and sutures were placed. Survival of animals was monitored and mean survival times calculated for each group given a specific inoculum of cells.

Temporal study of CNS-1 in rat brain with permanently-implanted cannulas for invasive characteristics

Anesthetized rats underwent one surgical procedure for the permanent implantation of a stainless steel cannula into right parietal brain (3 mm lateral to midline, 2 mm posterior to bregma, 4 mm depth)

as described [7]. The rats were allowed to recover from the surgery for at least one week before being further manipulated. Intracranial infusion of 10^6 CNS-1 tumor cells was given through the implanted cannula to rats in the awake state [9] and then sacrificed at 3–5 day intervals up to 22 days postinfusion. Brains bearing CNS-1 tumor were recovered and fixed in 10% buffered formalin. They were embedded in paraffin, serially sectioned and every thirtieth 5 μ section stained with hematoxylin and eosin for histopathological analysis.

Systemic study of CNS-1 invasiveness

To study the invasive characteristics of CNS-1 when given as a subcutaneous injection, 10^6 cells were implanted in the left hind flanks of animals. Tumor growth was observed for 120 days; then animals were sacrificed and necropsy performed.

Statistical analysis

Kaplan Meier survival curves were devised for each group as explained [14]. Mean survival times were calculated by Mantel-Haenzel nonparametric log-rank and Wilcoxon tests.

Table 1. Survival of rats given intracranial inocula of 9L and CNS-1 tumor cells

Number of cells	Mean survival time (days) ± SD	
	9L	CNS-1
1,000,000		20.5 ± 3.4
500,000		23.5 ± 3.5
100,000	23.3 ± 1.9	30.2 ± 5.5
50,000		29.6 ± 2.6
30,000	23.2 ± 1.6	
10,000	28.2 ± 4.5	
5,000	34.3 ± 3.3	
3,000	36.2 ± 7.4	
1,000	31.6 ± 3.1	
300	40.2 ± 5.3	

Titration of 9L gliosarcoma in Fischer 344 rats and CNS-1 glioma in Lewis rats. N = 6 for each group.

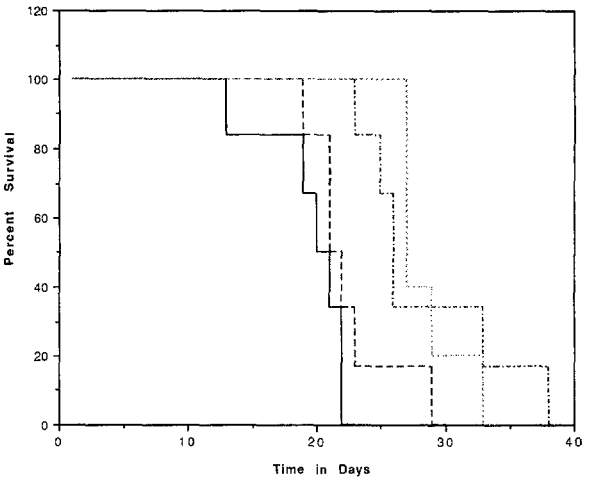

Fig. 1. Kaplan-Meier survival curves for the CNS-1 tumor-bearing groups where individual animals received inoculums of 10^6 (——), 5×10^5 (– – –), 10^5 (–·–·–), and 5×10^4 (.....) cells.

Results

The titration data on CNS-1 and 9L tumors cells are as given in Table 1. Lesser numbers of 9L cells are needed intracranially to produce lethal tumor growth in a given period than for CNS-1 tumor.

Kaplan-Meier survival curves for each group given a specific CNS-1 inoculum are shown in Fig. 1. The medians for each group are: 21.5 days for 10^6, 22.5 days for 5×10^5, 29 days for 10^5, and 28 days for 5×10^4.

CNS-1 and 9L cell lines were immunostained for neuroectodermal and other marker molecules, the results of which are listed in Table 2. The CNS-1 pri-

Table 2. Immunohistochemical staining of CNS-1 and 9L tumor cells

Marker antigen	CNS-1 cells	9L cells
glial fibrillary antigen protein	+	–
S100 protein	+/–	–
vimentin	++	–
neural cell adhesion molecule	+	+
retinoic acid receptor α	++	++
intercellular adhesion molecule-1	+	++
neuron specific enolase	+	+
neurofilament	–	–

Antibodies and sources used are listed in materials and methods. – no staining, +/– trace, + moderate intensity, ++ intense staining.

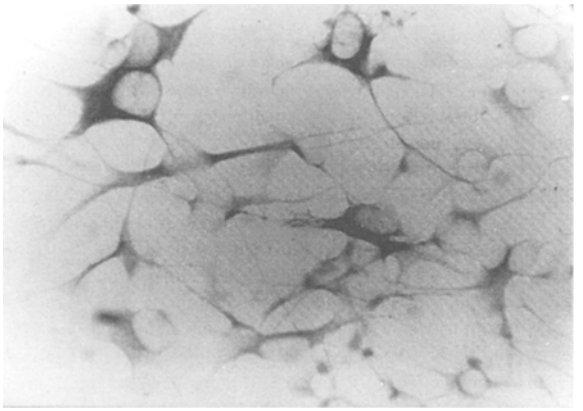

Fig. 2. Cultured CNS-1 cells staining positive for glial fibrillary acidic protein. × 1,200.

mary tumor as well as the tissue-cultured counterpart stains positively for the typical glial markers, glial fibrillary acidic protein (passage numbers up to 15) and S100 protein; 9L gliosarcoma is negative. Figure 2 shows the tissue cultured CNS-1 cells staining for glial fibrillary acidic protein. The CNS-1 cells also stain intensely positive for the primitive cell marker, vimentin, whereas 9L cells are negative. Both CNS-1 and 9L cells are positive for neural cell adhesion molecule, retinoic acid receptor α, intercellular adhesion molecule, and neuron specific enolase; both were negative for neurofilament.

Chromosomes from a Sprague-Dawley rat parotid cell line, 2RS, (Fig. 3A) were used for obtaining the normal karyotype and banding patterns; they closely match those from the idiogram drawn of rat chomosomes of the Norway rat, *Rattus norvegicus* [13]. Compared to the normal rat chromosome pattern, aberrancy is seen in both the CNS-1 and 9L tumor lines. Representative karyograms for the CNS-1 tumor line are shown (Figs 3B, 3C). The karyotypes are abnormal but relatively simple with a modal number of 42. There are one or more trisomies of either 11 or 13. Random losses of chromosomes occur and one marker chromosome is observed. In contrast, karyograms observed from several cells from the 9L gliosarcoma are rather complex (Figs 3D, 3E); it is impossible to assign a representative karyotype because of the complexity observed in individual cells; many duplicate chromosomes occur and as many as four copies of the same chromosome are obtained. The range of counts in the 9L cells counted is 56 to 66 (modal number = 62).

Gross coronal sections of brain from animals that succumbed from 9L gliosarcoma have a well demarcated tumor that essentially fills one hemisphere of brain (Fig. 4A). 9L shows only limited perivascular and leptomeningeal spread; areas of central necrosis and occasional hemorrhage could be seen within large cohesive tumor masses. In contrast, CNS-1 tumor locally and unilaterally infiltrates normal neuropil and widely extends bilaterally into distant parts of the brain by perivascular, periventricular and subarachnoid space (Fig. 4B).

A low power photomicrograph from the brain of a rat with 9L gliosarcoma (Fig. 5A) shows the well-demarcated border between tumor and normal brain and demonstrates compression at the interface. A higher power photomicrograph (Fig. 5B) shows highly undifferentiated, malignant spindle shaped cells with frequent mitotic figures.

A low power photomicrograph from the brain of a rat with CNS-1 tumor (Fig. 6A) demonstrates perivascular spread and individual neoplastic cell permeation of brain parenchyma. Higher power photomicrographs from the same CNS-1-bearing brain shows perivascular localization of tumor (Fig. 6B) and mitotically active, individual tumor cells growing near the ventricular surface (Fig. 6C) with some individual neoplastic cell permeation of brain parenchyma. Where CNS-1 formed a more cohesive mass in leptomeninges, cystic formation was sometimes seen (Fig. 6D).

Animals receiving intracranial 10^6 CNS-1 tumor cells were sacrificed at 3–5 days intervals after infusion into right parietal cortex. The glioma-bearing brains were subjected to histopathological screening for an assessment of the infiltrative patterns of the tumor. Individual cell permeation was more apparent with CNS-1, both at early and at later time points, than in 9L. Parenchymal infiltration of CNS-1 usually did not extend beyond one hemisphere nor was there a particular proclivity for involvement of white matter bundles such as the anterior commissure or corpus callosum. In late stage disease, compared to 9L gliosarcoma, CNS-1 showed more extensive leptomeningeal, perivascular, and periventricular spread.

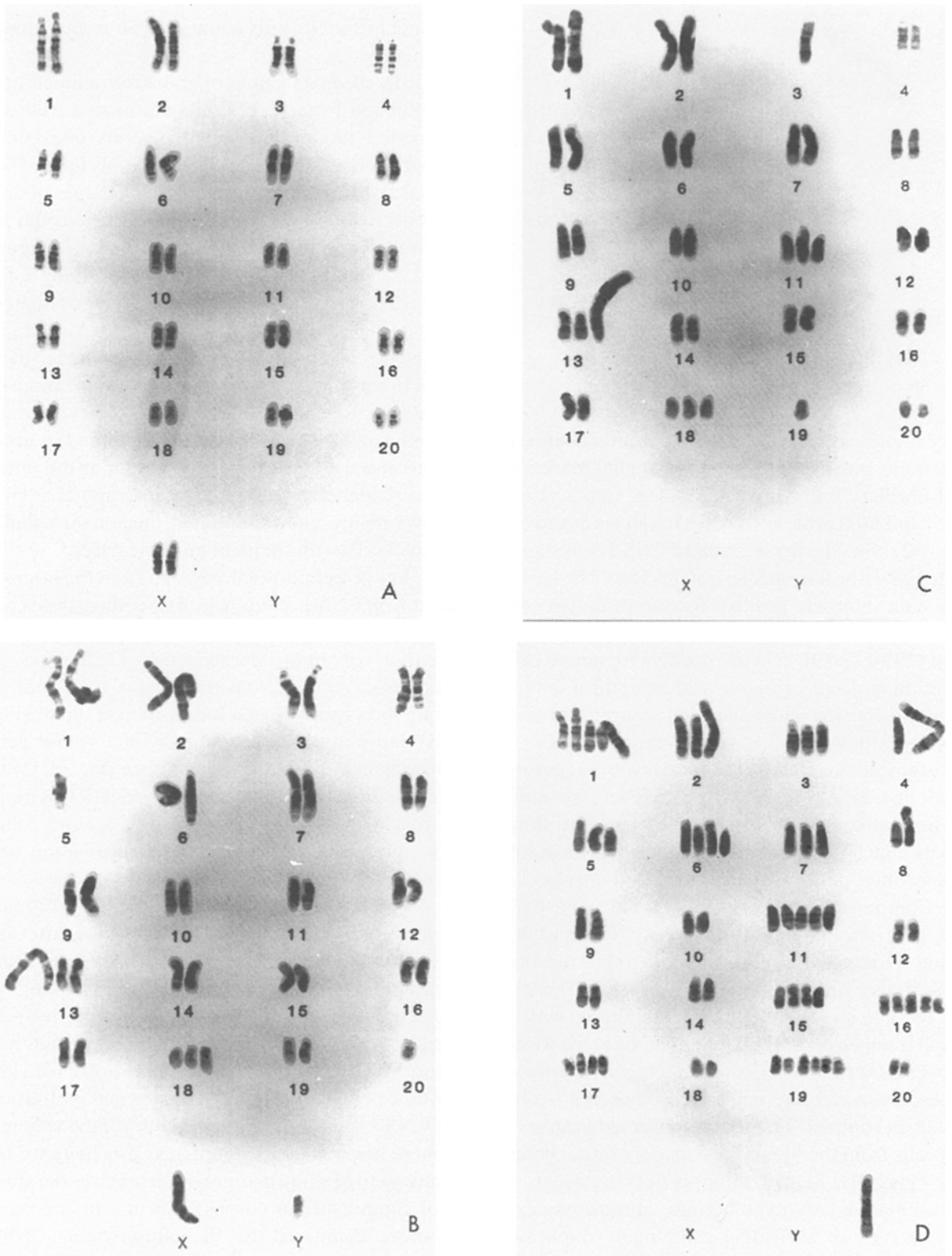
1
2
3
4
5
6
7
8
9
10
11
12
13
14
15
16
17
18
19
20
X
Y
A
1
2
3
4
5
6
7
8
9
10
11
12
13
14
15
16
17
18
19
20
X
Y
C
1
2
3
4
5
6
7
8
9
10
11
12
13
14
15
16
17
18
19
20
X
Y
B
1
2
3
4
5
6
7
8
9
10
11
12
13
14
15
16
17
18
19
20
X
Y
D

Fig. 3.

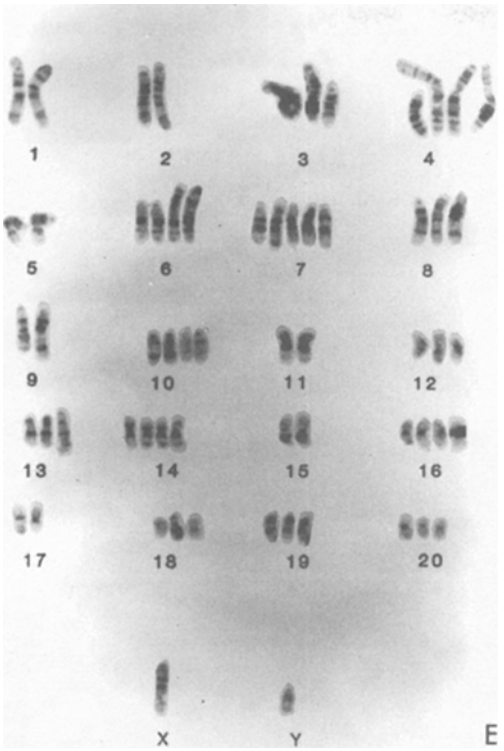

Fig. 3. Chromosomes from a Sprague-Dawley rat parotid cell line, 2RS, show a normal karyotype (A), representative karyograms from the CNS-1 tumor cell line (B, C), and karyograms from several 9L gliosarcoma cells (D, E).

Lewis rats given subcutaneous injections of CNS-1 tumor in the flank or thigh were sacrificed at 120 days postinjection. The tumor caused massive local tissue distention but the animals did not suc-

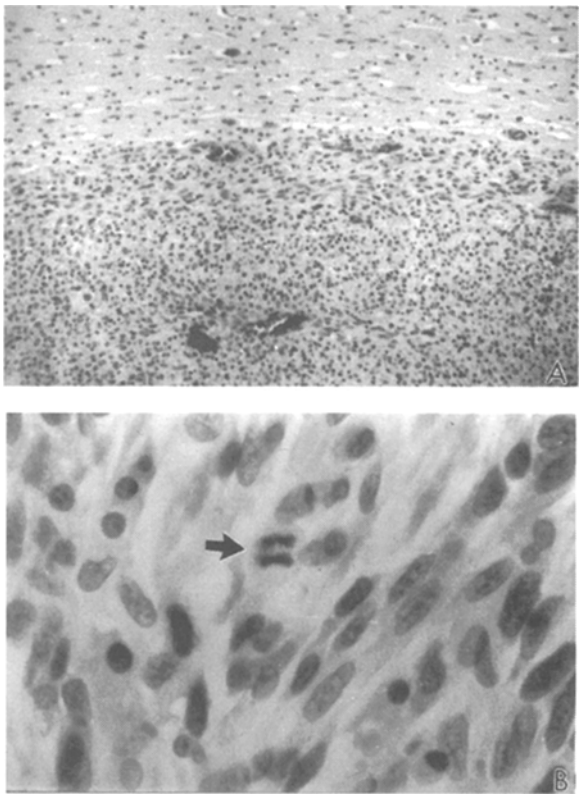

Fig. 5. Low power photomicrograph from the brain of a rat with 9L gliosarcoma (A) showing the well-defined border between tumor and normal brain and demonstrating compression at the interface. Higher power photomicrograph (B) from the same 9L tumor-bearing brain shows the highly undifferentiated, malignant nature of this experimental tumor line. Mitotic figures (arrow) are commonly seen within this cohesive spindle cell tumor. Hematoxylin-eosin stained. (A) × 144 (B) × 360.

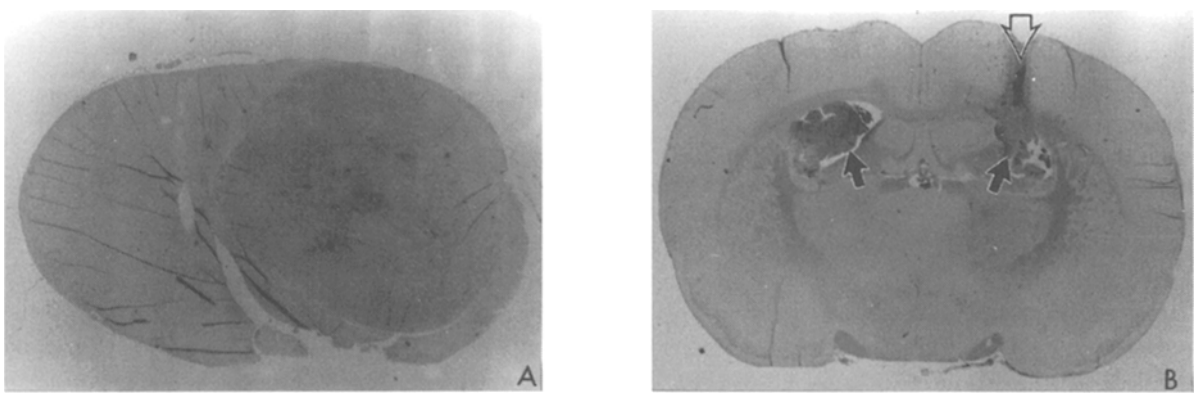

Fig. 4. Gross coronal section of brain from an animal succumbing to 9L gliosarcoma (A) shows a well demarcated tumor that essentially fills one hemisphere and causes significant midline shift. Central hemorrhage and necrosis is commonly seen. Coronal section from the brain of a rat succumbing to CNS-1 glioma (B). The CNS-1 tumor spreads throughout the ventricles with frond-like expansion of the choroid plexus stroma (solid arrows). The instillation site is also evident at this level (open arrow). Hematoxylin-eosin stained. (A, B) × 36.

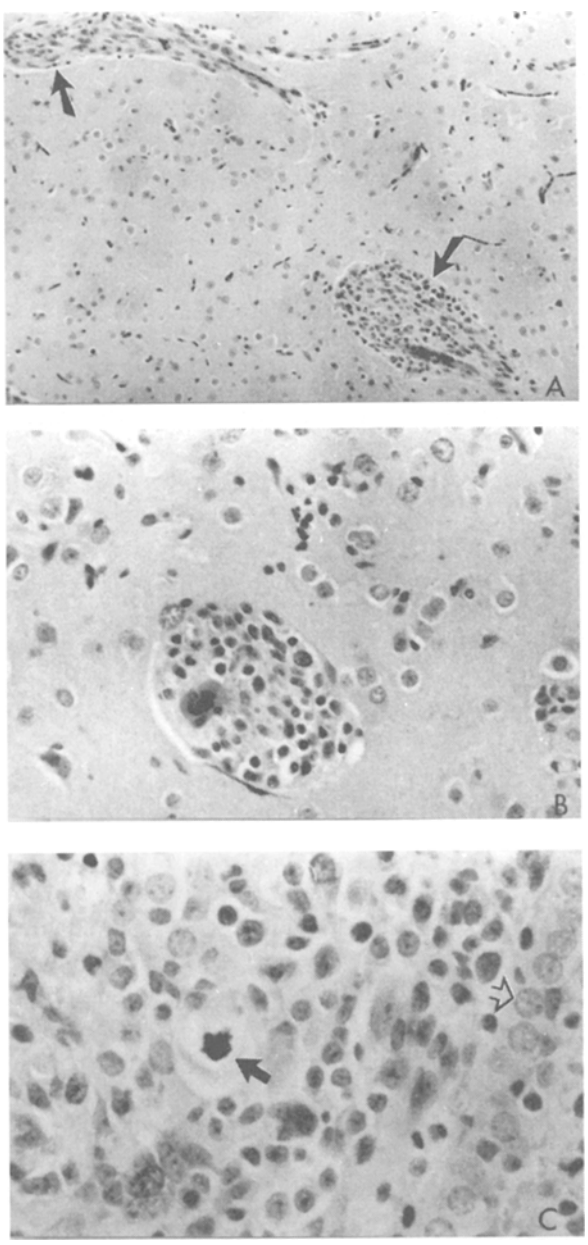

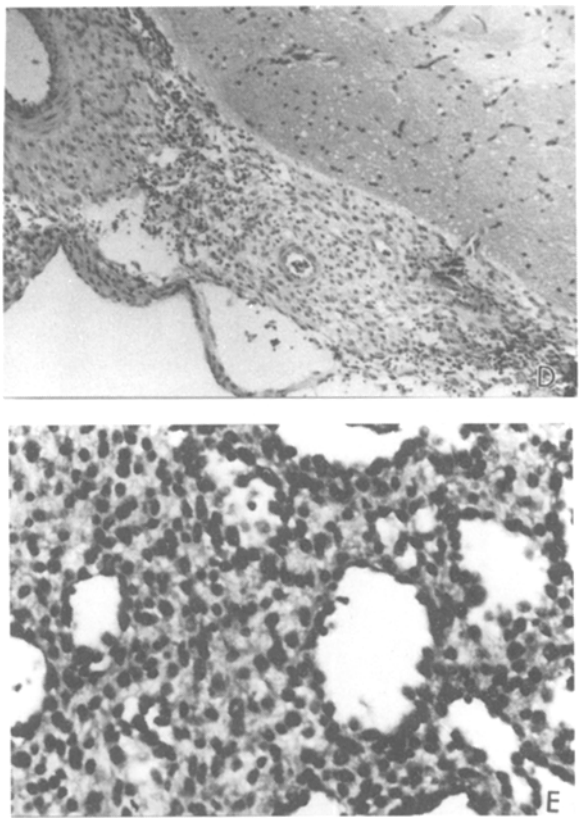

Fig. 6. Low power photomicrograph from the brain of a rat with CNS-1 tumor (A) demonstrating perivascular spread (arrow) and more individual neoplastic cell permeation of brain parenchyma than is seen with 9L. High power photomicrographs from the same CNS-1 bearing brain showing perivascular localization (B), individual tumor cells growing near the ventricular surface (C, see arrowheads for ependymal cell lining) with individual neoplastic cell permeation of brain parenchyma, some undergoing mitoses (arrow). Where CNS-1 occasionally forms a cohesive tumor mass in the leptomeninges, cystic degeneration in the tumor is seen (D). Cystic degeneration is also present in CNS-1 tumor growing subcutaneously (E). Hematoxylin-eosin stained. (A, D) × 144 (B, C, E) × 360.

cumb to the tumor. Autopsy of the animals revealed that the tumor remained at the site of injection and did not metastasize. Tumor formed a relatively cohesive mass in muscle with only limited infiltration between individual muscle fibers. Cystic degeneration was seen centrally in the tumor mass (Fig. 6E), similar to that seen in cohesive tumor masses in the central nervous system (Fig. 6D). Histologically the tumor was identical in muscle to that in the central nervous system.

Discussion

One difficulty in testing immunotherapeutic modalities for any neoplasm lies in choosing an appropriate experimental system that mimics the human situation. Immunotherapy, if it is to succeed, must identify normal self while destroying tumorous self. If the experimental tumor is non-self, i.e., it is not totally MHC compatible with the host animal, then the immunological mechanism which could cause it

to be destroyed might have absolutely no significance to treating brain neoplasms in man. The underlying immunological mechanism in such an experimental model may merely be graft rejection (elimination of non-self tissue) and not any antineoplastic immunological effect. Human patients are suffering from a tumor that arose from their own tissues; they will not eliminate it via the mechanism of allogeneic graft rejection. Therefore, we legitimately questioned whether an appropriate experimental system was available to study immune regimens for the treatment of human gliomas.

In the rat, most available glial tumor models were either derived from outbred animals, have been in tissue culture for decades, and/or are very poor mimics of the growth and spread of typical human gliomas. With the potential of antigenic drift to occur over time in inbred rats from isolated colonies, the success of any given immunotherapeutic regimen tested today could be held in question. For these reasons, we decided to induce and characterize a new astrocytic neoplasm with useful characteristics in an inbred, immunologically characterized rat strain.

In this study, decreased numbers of 9L cells in relation to CNS-1 cells were needed to produce lethality in a given period in the rat. This is probably reflective of the malignant phenotypes of 9L, its sarcomatous nature, and its ability to grow as a well-circumscribed, spheroidal mass which produces mass effect in the animal. In our system only limited local perivascular and subarachnoid spread was seen with 9L. Others have documented that 9L tumor adjacent to the instillation site and main tumor mass invades parenchyma by periventricular and perivascular routes [15]. 9L in our hands better simulated a human brain metastasis or sarcoma than a human glioma. In contrast, the CNS-1 glial tumor cells had fewer predictable chromosomal abnormalities, infiltrated normal neuropil, leptomeninges and perivascular space and was less well circumscribed. The animals probably died because of tumor growth in a critical center(s) of the brain, rather than by mass effect as in the 9L model.

The diffuse pattern exhibited by CNS-1 in animals at death more clearly resembles a human glioblastoma multiforme [16] than does the more cohesive mass seen with 9L. The invasive pattern of CNS-1 in early and late stage disease showed a high degree of leptomeningeal, periventricular, perivascular spread in addition to individual tumor cell permeation of parenchyma. While the extensive leptomeningeal spread observed may be partially an artifact of the infusion itself [17], we used identical infusion mechanism for 9L and CNS-1, and 9L showed less such spread.

Overall, the CNS-1 brain tumor model closely simulates growth and histochemical characteristics of human malignant gliomas. The model meets both genetic and infiltrative glial simulation requirements for ideally testing adoptive immunotherapy regimens *in vivo,* and as such, seems superior for such trials when contrasted with the 9L gliosarcoma model. Moreover, since it is accepted without rejection in non-central nervous system sites by inbred Lewis rats, it should provide an excellent model in which to investigate a variety of immunological therapeutic modalities.

Acknowledgements

We acknowledge the technical expertise of Mr. Dan LiButti, Ms. Kimberly Ricketts and Ms. Joanna Bruno; Ms. Holly Terry and Mr. Joel Doub, both supported by Summer Cancer Student Fellowships, participated in the animal experiments. We thank Dr. Helvise Morse of the University of Colorado Cancer Center, Cytogenetics Core for the karyotypic analyses. This work was supported in part by National Institutes of Health Grants RO1-NS28905 and KO4-NS01401 to CAK and RO1-NS27321 to WFH, and The Ride for Kids Foundation. CAK is a member of the University of Colorado Cancer Center and is a recipient of an NIH Research Career Development Award. The Histopathology and Cytogenetics Core Facilities of the Colorado Cancer Center were utilized.

References

1. Laws ER Jr, Thapar K: Brain Tumors. Cancer 43: 263–271, 1993

2. Crafts D, Wilson CB: Animal models of brain tumors. Natl Cancer Inst Monogr 46: 11–17, 1977
3. Benda P, Someda K, Messer J, Sweet WH: Morphological and immunochemical studies of rat glial tumors and clonal strains propagated in culture. J Neurosurg 34: 310–323, 1971
4. Blume MR, Wilson CB, Vasquez DA: Immune response to a transplantable intracerebral glioma in rat. In: Sane K, Ishii S, LeVay D (eds) Recent Progress in Neurological Surgery, Excerpta Medica, Amsterdam, 1974, pp. 129–132
5. Mahaley MS, Gillespie GY: Immunotherapy of patients with glioma: fact, fancy and future. Prog Exp Tumor Res 28: 118–135, 1984
6. Kruse CA, Lillehei KO, Mitchell DH, Kleinschmidt-DeMasters BK, Bellgrau D: Analysis of interleukin 2 and various effector cell populations in adoptive immunotherapy of 9L rat gliosarcoma: allogeneic cytotoxic T lymphocytes prevent tumor take. Proc Natl Acad Sci (USA) 87: 9577–9581, 1990
7. Kruse CA, Mitchell DH, Kleinschmidt-DeMaster BK, Bellgrau D, Eule JM, Parra JR, Kong Q, Lillehei KO: Systemic chemotherapy combined with local adoptive immunotherapy cures rats bearing 9L gliosarcoma. J Neuro-Oncology 15: 97–112, 1993
8. Redd JM, Lagarde A-C, Kruse CA, Bellgrau D: Allogeneic tumor-specific cytotoxic T lymphocytes. Cancer Immunol Immunother 34: 349–354, 1992
9. Fleshner M, Watkins LR, Redd JM, Kruse CA, Bellgrau D: A 9L gliosarcoma transplantation model for studying adoptive immunotherapy into the brains of conscious rats. Cell Transplantation 1: 307–312, 1992
10. Kruse CA, Schiltz PM, Bellgrau DB, Kong Q, Kleinschmidt-DeMasters BK: Intracranial administration of single or multiple source allogeneic cytotoxic T lymphocytes: chronic therapy for primary brain tumors. J Neuro-Oncology 19: 161–168, 1994
11. Kruse CA, Mitchell DH, Kleinschmidt-DeMasters BK, Franklin WA, Morse HG, Spector EB, Lillehei KO: Characterization of a continuous human glioma cell line DBTRG–05MG: growth kinetics, karyotype, receptor expression, and tumor suppressor gene analyses. *In Vitro* Cell Dev Biol 28A: 609–614, 1992
12. Hickey WF, Gonates NK, Kimura H, Wilson DB: Immunohistochemical identification and quantitation of lymphocytes infiltrating the spinal cords of Lewis rats with experimental allergic encephalomyelitis. J Immunol 131: 2805–2809, 1983
13. Gallimore PH, Richardson CR: An improved banding technique exemplified in the karyotype analysis of two strains of rat. Chromosoma, Berl 41: 259–263, 1973
14. Brown BW Jr, Hollander M: Statistics: A Biomedical Introduction. Wiley and Sons, New York, 1977, pp. 343–346
15. Lampson LA, Wen P, Roman VA, Morris JH, Sarid JA: Disseminating tumor cells and their interactions with leukocytes visualized in the brain. Cancer Res 52: 1018–1025, 1992
16. Burger PC, Schiethauer BW, Vogel SS: Surgical pathology of the nervous system and its coverings. Churchill, Livingston, New York, NY, 1991, p. 234
17. Pedersen P-H, Marienhagen K, Mork S, Bjerkvig R: Migratory pattern of fetal rat brain cells and human glioma cells in the adult rat brain. Cancer Res 53: 5158–5165, 1993

Address for offprints: C.A. Kruse, University of Colorado Health Sciences Center, Department of Surgery, Campus Box C307, 4200 East 9th Avenue, Denver, CO 80262, USA